Physica A 410 (2014) 9–16

Contents lists available at ScienceDirect

Physica A

journal homepage: www.elsevier.com/locate/physa

Effects of non-stationarity on the magnitude and sign scaling in the multi-scale vertical velocity increment

Qinglei Li, Zuntao Fu *, Naiming Yuan, Fenghua Xie

Lab for Climate and Ocean–Atmosphere Studies, Department of Atmospheric and Oceanic Sciences, School of Physics, Peking University, Beijing, 100871, China

HIGHLIGHTS

- No significant scaling range for original stationary records.
- Nonlinear correlation is obvious in increment records for both cases.
- Two scaling ranges in both magnitude and sign fluctuations exist with larger lag.

ARTICLE INFO

Article history:
Received 8 November 2013
Received in revised form 4 March 2014
Available online 10 May 2014

Keywords:
Scaling
Non-stationarity
Magnitude
Sign
Multi-scale increments

ABSTRACT

We study the scaling properties of multi-scale increment series from the stationary and non-stationary vertical velocity records by the detrended fluctuation analysis (DFA) and series decomposition methods, and show the impact of non-stationarity on the magnitude and sign scaling properties. Firstly, we show it is difficult to define a significant scaling range for stationary records themselves. Secondly, for increment series with lag one, the nonlinear correlation found in magnitude fluctuation (i.e. volatility fluctuation) is obvious for both cases. And over the smaller scale range, the linear correlation found usually in the sign series is the same for both cases. However, over the larger scale range, the difference is sharp and marked nonlinear correlation is also incorporated for the non-stationary sign series. Thirdly, with the lags in increment increasing, there exist two scaling ranges in both the magnitude and sign fluctuations. The nonlinear correlation in the magnitude series over both small and large scale ranges decreases with the lags increasing. For the sign series, the linear correlation is dominant over both small and large scale ranges for stationary case; however, the nonlinear correlation can be found over the large scale ranges for non-stationary case and will decrease with lags increasing. The nonlinear correlation found in the sign series over large-scale range is resulted from the modulation of the large scale structures found in the non-stationary data, which will incorporate parts of the magnitude information into the sign series.

1. Introduction

A broad class of physical and geophysical systems exhibits complex dynamics, which is associated with the presence of many components interacting over a wide range of time or space scales. These often-competing interactions may generate an output signal with fluctuations that appear "noisy" and "erratic" but reveal scale-invariant structure [1]. To address this problem, one of the most commonly used methods, detrended fluctuation analysis (DFA) was developed to accurately

* Corresponding author. Tel.: +86 010 62767184.
E-mail address: fuzt@pku.edu.cn (Z. Fu).

http://dx.doi.org/10.1016/j.physa.2014.05.004
0378-4371/

quantify long-range correlations embedded in time series through their scaling exponents [2,3]. Long-range correlations are usually characterized by scaling laws where the scaling exponents quantify the strength of these correlations [4]. It has been successfully applied to diverse fields such as DNA sequences [5], heart rate dynamics [6], neuron spiking [7], human gait [8], long-time weather records [9–11], geology [12], cloud structure [13], ethnology [14], economic time series [15], and solid state physics [16].

Some previous studies [17–19] have investigated the correlation of wind velocity records collected within the atmospheric boundary layer. Carefully inspecting the results given by these authors, it can be easily found that there is no dominant scaling range from the original wind velocity records [17,18], so the fitted exponents over an insignificant scaling range are with great uncertainty. Actually, we cannot find a significant scaling range for stationary vertical wind velocity records. The significant scaling range exists in DFA results of the volatility series (i.e. magnitude series of one step ahead velocity increment) of wind velocity series collected in the atmospheric boundary layer [19]. Govindan and Kantz reported the volatility scaling results from volatility series and found that nonlinear correlation does not necessarily imply multi-fractality. However, there still exist two problems unresolved. The first one is how much the results will be changed when lags in the velocity increment increase, since the multi-scale lags have been often used in the structure function analysis of turbulent wind velocity. The second one is how to quantify the effect resulted from the non-stationarity found in the wind velocity series collected in the atmospheric boundary layer, especially its impact on the nonlinear correlation.

The motions within the atmospheric boundary layer are inherently non-stationary. Non-stationarity usually means the average, standard deviation, and higher moments or the correlation functions are not invariant under time translation [20]. As an important aspect of complex variability, it can often be associated with different trends in the record or heterogeneous segments (patches) with different local statistical properties [20]. Turbulence series collected in the atmospheric surface layer over land may often be non-stationary. It has been found that a stationarity test shows that about 40% of the turbulent heat fluxes at Summit, Greenland are classified as non-stationary [21]. Mahrt and Thomas examined the relationship of turbulence to the non-stationary wind and stratification, and found that the turbulence is simultaneously generated by different non-stationary mechanisms [22]. Using telegraph approximation [23,24]), we have found that non-stationary records possess different cluster and intermittency properties from those of its stationary counterparts [25]. Other techniques for detection of correlations like the autocorrelation function and the power spectrum are not suited for non-stationary time series. The effects of non-stationarity cannot be quantified by the probability density function (PDF) and the spectral analysis of the original series [25]. However, the PDF of the multi-scale wind velocity increments shows different features for stationary and non-stationary series and the differences can be quantified by multi-scale entropy analysis [26]. Since one advantage of the DFA method is to avoid spurious detection of correlations caused by the non-stationarity in the series, how to use DFA to quantify the effect that resulted from the non-stationarity found in the wind velocity series collected in the atmospheric boundary layer, especially its impact on the nonlinear correlation, deserves further studies.

Firstly, we use the space time-index method (STI) to classify different vertical velocity records as two kinds, stationary or non-stationary. The STI is a graphical method, and can be effectively used to detect dynamical non-stationarity in time series [27]. Detailed descriptions of the STI method can be found in Refs. [28,29] and are not repeated here. Secondly, since the observable variables in the output of natural systems at each moment are the product of its magnitude and sign [30,1,6,31–36], we focus on the sign and magnitude series of the velocity increment with lag one and obtain the correlations within significant scaling range for both stationary and non-stationary series. Thirdly, we confirm that different nonlinearity correlations exist in stationary and non-stationary series using the phase randomized surrogate method (PRS, [37]). Lastly, the magnitude and sign fluctuations of multi-scale increment from vertical velocity records are investigated to quantify the correlation variation with lags increasing.

The rest of the paper is organized as follows. In Section 2, we will make a short introduction of the analysis methods and the data sets used in this paper. Results for the magnitude and sign scaling from multi-scaled increment of stationary and non-stationary turbulent velocity series are provided in Section 3. In Section 4, we make a brief discussion and some conclusions are summarized.

2. Data and methodology

2.1. Data

In this paper, atmospheric boundary-layer turbulence records collected during the experiment in Huaihe River Basin (HUBEX) between June 5 and June 22 in 1998 are used in the analysis. Huaihe River basin is situated between Yangtze River and Yellow River with a total area of 270,000 km^2. It represents the typical climate condition in the East Asia monsoon region, and effects of human activity are relatively slight. The observation site was in the yard of the Shouxian Meteorological Observatory in Anhui province, People's Republic of China and is located on the western edge of a large rice field. The yard was about 200 m long in the north–south direction. The measurement height was set as 4 m above ground, a three-dimensional sonic anemometer (SAT-211/3 K, sample rate 20 Hz, sound path 0.15 m) was used to measure wind velocity components and temperature, and each hour sampling will be taken as one record (detailed information can be found in the Refs. [38,39]). And this data set has been applied to analyze the characteristics of turbulence in the atmospheric boundary-layer, and nonlinear features have been derived [40,38,39,41]. Typical parts of records can be found in Fig. 1,

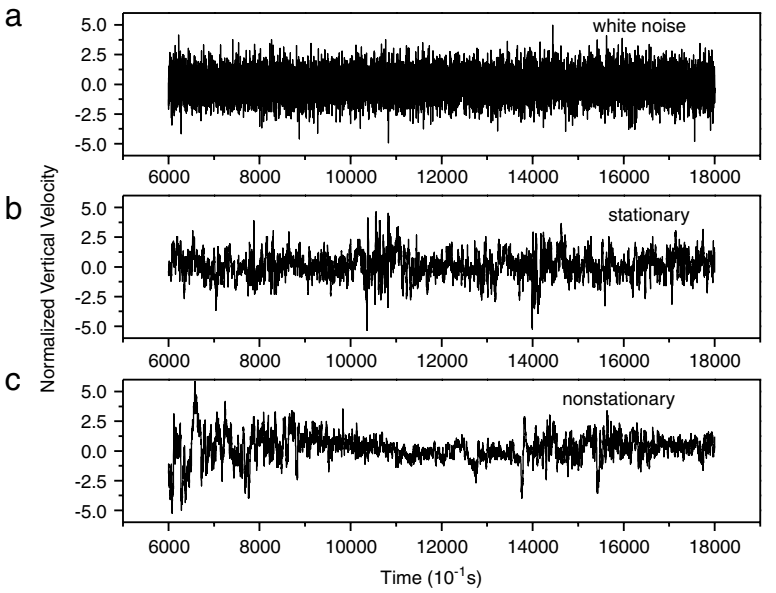

Fig. 1. Segments of the normalized (subtracting the mean and divide by the standard deviation) original stationary and non-stationary vertical velocity series, with normalized white noise for reference.

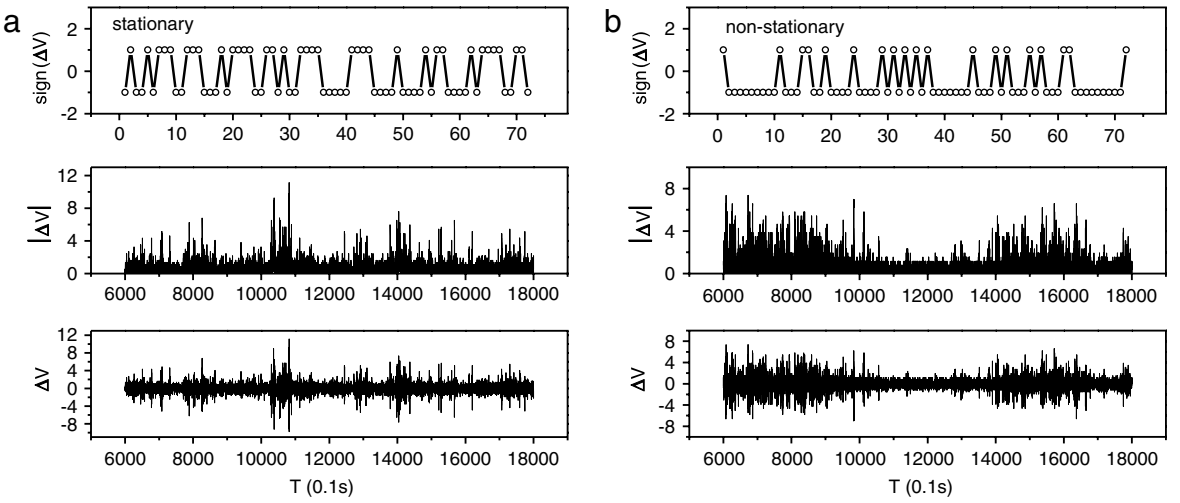

Fig. 2. The velocity increment series, magnitude series and sign series for (a) stationary and (b) non-stationary vertical velocity series.

where stationary and non-stationary records show different features, especially there are dominant larger scale structures in the non-stationary record, see Fig. 1(c).

For the chosen stationary and non-stationary series V_i' in Fig. 1(b) and (c), we calculate the multi-scale increment series $\Delta V = V'(i+n) - V'(i)$ obtained from records of velocity fluctuations $V'(i)$, where i indexes each velocity fluctuation and $n = 2^h$ stands for multi-scale time lags with $h = 0, 1, 5, 10$. Then we decompose the increment series into a magnitude series $|\Delta V|$ and a sign series $\mathrm{sign}(\Delta V)$: $\Delta V = \mathrm{sign}(\Delta V) * |\Delta V|$; for $n = 1$ the magnitude series is also called the volatility series. For $n = 2^0 = 1$ the increment series ΔV, the magnitude series $|\Delta V|$ and the sign series $\mathrm{sign}(\Delta V)$ are shown in Fig. 2 for (a) stationary and (b) non-stationary respectively.

2.2. Methodology

2.2.1. Detrended fluctuation analysis method (DFA)

DFA involves the following steps: firstly, consider a fluctuating record x_i ($i = 1, 2, 3 \ldots N$). Calculate the random walk profile by integrating the signal, $Y(i) = \sum_{k=1}^{i} (x_i - \langle x \rangle)$, where $\langle x \rangle$ is the mean of x_i. Secondly, divide the profile into N_s non-overlapping boxes of equal length s, where $N_s = [N/s]$. The same procedure is repeated from the other end of the

record since the length of the record is not always a multiple of s, and we get $2N_s$ boxes altogether. In each box of length s, the local trend was calculated by fitting the data using a polynomial p_v^k of order k. Thirdly, we detrend the integrated time series $Y(i)$, by subtracting the local trend p_v^k, where $v = 1, 2, \ldots, 2\,N_s$, $Y_s = Y\,(i) - p_v^k$ and calculate the variance function

$$F_s^2\,(v, s) = \langle Y_s^2(i)\rangle = \frac{1}{s}\sum_{i=1}^{s} Y_s^2\,[(v-1)\,s + i] \tag{1}$$

in each box. The root-mean-square fluctuation of this integrated and detrended time series $F_s^2\,(v, s)$ is calculated by $F\,(s) = \left[\frac{1}{2N_s}\sum_{v=1}^{2N_s} F_s^2\,(v)\right]^{1/2}$. For the case of long-term power-law correlations, $F\,(s)$ will increase with the increase of s, as a power law $F\,(s) \sim s^{\alpha}$. For the type of uncorrelated data, the integrated value $Y(i)$ corresponds to a random walk; and therefore $\alpha = 0.5$ [2]. The α greater than 0.5 and less than or equal to 1.0 indicates persistent long-term power-law correlations such that a large (compared to the average) value of x_i is more likely to be followed by large x_{i+1} and vice versa [42]. In contrast, $0 < \alpha < 0.5$ indicates a different type of power-law correlation such that large and small values of the time series are more likely to alternate. A special case of $\alpha = 1$ corresponds to $1/f$ noise. For $\alpha > 1$, correlations exist but cease to be of a power-law form; $\alpha = 1.5$ indicates Brown noise, the integration of white noise. Notice the relationship between the DFA exponent α and the spectrum exponent is $\beta = 2\alpha - 1$, and the connection DFA exponent α with the autocorrelation function exponent γ is $\gamma = 2\,(1-\alpha)$ [9].

2.2.2. Phase-randomized surrogate method (PRS)

In order to confirm the nonlinearity in the wind velocity magnitude and sign series, we perform the phase-randomized surrogate method (PRS) for the increment series [37]. After PRS, both the long-range power-law autocorrelations and the long-range cross-correlation function vanish [43]. PRS involves the following steps: firstly we perform a Fourier transform on a velocity fluctuation increment time series, preserving the amplitudes of the Fourier transform but randomizing the Fourier phases. Then we perform an inverse Fourier transform to create a surrogate series. This procedure eliminates nonlinearities, preserving only the linear features (i.e., two-point correlations) of the original time series [1]. After PRS, we study the long-term correlations in magnitude and sign series of the surrogated series by using DFA to calculate the scaling exponent α_{PRS}. Since phase-randomized surrogate destroys the nonlinear correlations, the scaling behavior will change after PRS if nonlinearity exists in the considered magnitude or sign series. We define $\Delta\alpha = \alpha - \alpha_{\mathrm{PRS}}$ as the change of scaling exponent after PRS to quantify the strength of nonlinear intensity.

3. Results

3.1. Non-stationary characteristics and scaling exponents

First of all, we can see the obvious difference between the stationary and non-stationary turbulent vertical wind velocity records from the observational series directly, see Fig. 1. There is more dominant large scale structures in the non-stationary ones and these kinds of large scale eddies can also be found in their increment, magnitude and sign series as shown in Fig. 2. The other descriptive difference between two groups is that there are more large fluctuations in the non-stationary wind velocity increment, see Fig. 2(b).

Fig. 3 shows the scaling behavior of the stationary and non-stationary vertical wind velocity records themselves in log–log plot, with white noise ($\alpha = 0.5$) for reference. The log–log plot for the stationary series is not linear but fitted by a parabola function $\log F\,(s) \sim -0.24(\log s)^2 + 2.14\log s - 3.36$. The slope α of the fluctuation functions changes gradually with window size for the stationary series. There is no significant scaling range for the stationary series. For the non-stationary series the scaling region is partitioned into two regions around $s = s_x$. In the smaller range $s < s_x$, the scaling exponent is 1.45, and in the larger scaling range $s > s_x$ the scaling exponent is 0.89. These represent what is called "local scaling exponents" [17]. Thus, the "crossover" from one scaling exponent (1.45) to the other (0.89) is seen to occur approximately at a time scale $s = s_x \approx 30$ s. A crossover usually arises due to changes in the correlation properties of the signal at different scales [44]. At short time scales ($s < 30$ s), the data exhibits behavior similar to Brown noise ($\alpha = 1.45$), whereas for longer time scales ($s > 30$ s) one observes persistent long-range correlations ($\alpha = 0.89$). After shuffling the stationary and non-stationary time series, all the scaling exponents α drop to 0.5, same as those of white noise.

3.2. Correlation analysis of magnitude and sign series

The comparative scaling behaviors of magnitude series (volatility series) are shown for stationary and non-stationary vertical velocity series in Fig. 4(a). Contrary to scaling analysis of the velocity records themselves, there exists a wider significant scaling range for both stationary and non-stationary cases. Previous studies have demonstrated that information about nonlinear properties of flow dynamics can be quantified by long-range power-law correlation in magnitude of the increments [1,31], so the different magnitude scaling exponents exhibit different nonlinear dynamics in the two kinds of velocity time series. For the stationary, the scaling exponent is 0.77 within the whole range, while the scaling exponent

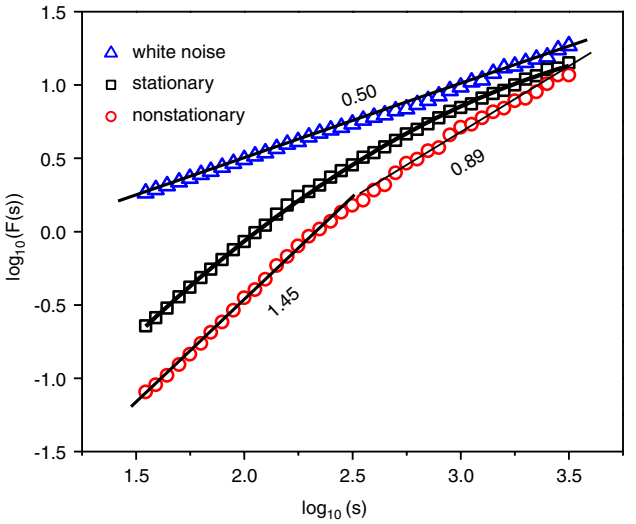

Fig. 3. The scaling behaviors of the original stationary and non-stationary vertical velocity series, with white noise for reference.

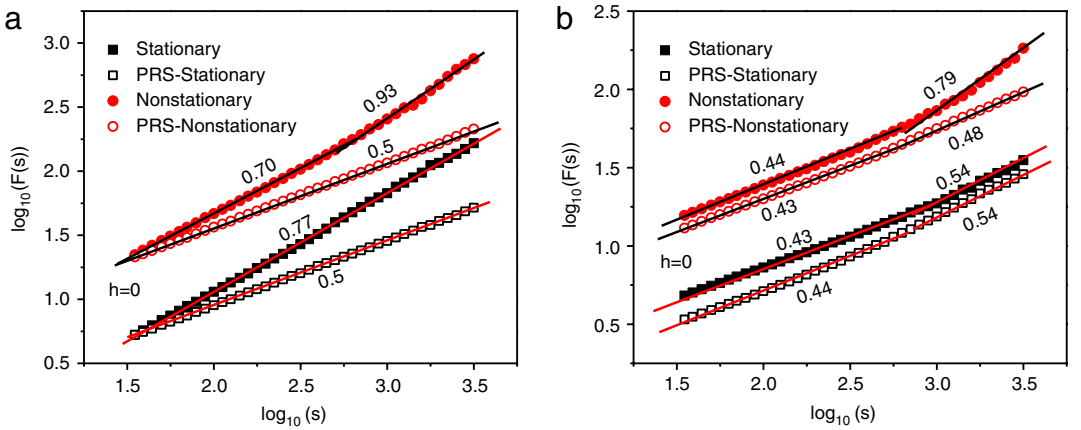

Fig. 4. The DFA results for the stationary and non-stationary increment velocity traces as well as their phase randomized surrogate counterparts, (a) for the magnitude series, (b) for the sign series.

changes from $\alpha_1 = 0.70$ to $\alpha_2 = 0.93$ as the time scale increases and the crossover happens at a time scale $s = s_x \approx 75$ s for the non-stationary one. For both stationary and non-stationary cases, there are predominant nonlinear correlations. Our results for stationary series are consistent with results from Govindan and Kantz, who have showed wind speed volatility is long-range correlated with an exponent $\alpha = 0.7 \pm 0.04$ within a range of 2 min to 1.5 h [19]. However, the crossover shown in Fig. 4(a) for the non-stationary series is first discovered here. For convenience, we define α_1 as the scaling exponent over the small scaling range $s < s_x$, and α_2 as the scaling exponent over the larger scaling range $s > s_x$, regardless of the value of the crossover s_x, see Table 1.

Fig. 4(b) shows the different scaling behaviors of sign series for stationary and non-stationary vertical velocity series. Contrasted with long-range positive correlations in the magnitude series at all scales in Fig. 4(a), anti-correlations (Fig. 4(b)) are found in the sign time series at small scales with α around 0.4 and long-range positive correlations ($\alpha = 0.79$) occur in the sign series at large scales just for non-stationary cases. Previous studies have shown that the sign series from the increments of the original signal contain linear correlation information about the underlying dynamics [1]. The anti-correlated behavior of sign series at small scales reflects that large and small values of the original time series are more likely to alternate. However, at large scales the long-range positive correlations indicate that large and small values of the original time series are more likely to clustered for the non-stationary cases; this is a significant difference between these two types of time series.

Since phase-randomized surrogate destroys the nonlinear correlations, the scaling behavior will change after PRS if nonlinearity exists in the considered time series. Ashkenazy has shown the sign series are mainly related to linear properties of the original series [1,31]. Here, for the considered sign series of non-stationary traces, the scaling exponent changes from 0.79 to 0.48 after PRS ($\Delta\alpha = 0.31$ see Table 1). That is to say the sign series show clustering property and also contain

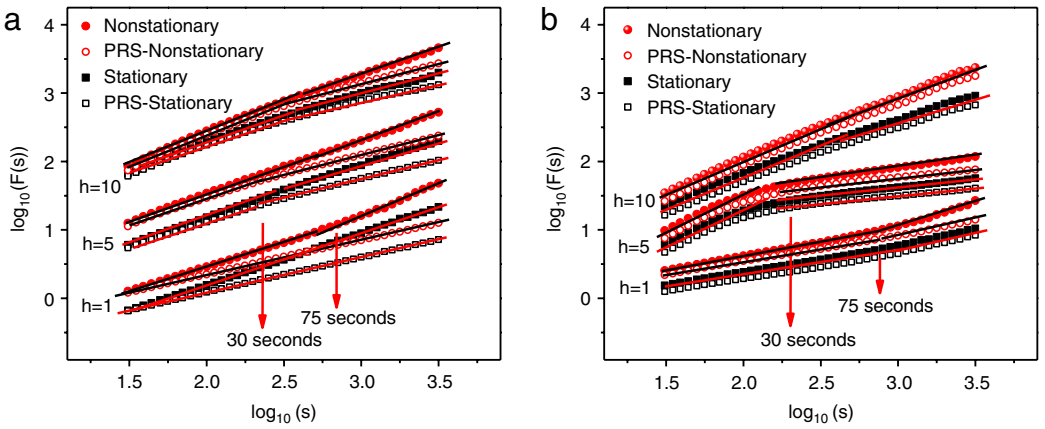

Fig. 5. The DFA results for the multi-scale increment of stationary and non-stationary velocity traces as well as their phase randomized surrogate counterparts, with $h = 1, 5, 10$ from bottom to top. (a) For the magnitude series, (b) for the sign series.

Table 1
The magnitude and sign scaling exponents for the multi-scale increment of stationary (STA) and non-stationary (NON) vertical velocity series. We define $\Delta\alpha$ as the change of scaling exponent after PRS, α_1 as the scaling exponent over the small scale range $s < s_x$, and α_2 as the scaling exponent over the large-scale range $s > s_x$, regardless of the value of the crossover s_x.

Time series	Scale factor	Magnitude						Sign					
		α_1			α_2			α_1			α_2		
		Origin	PRS	$\triangle\alpha_1$	Origin	PRS	$\triangle\alpha_2$	Origin	PRS	$\triangle\alpha_1$	Origin	PRS	$\triangle\alpha_2$
STA	$h = 0$	0.77	0.50	0.27	0.77	0.50	0.27	0.43	0.44	−0.01	0.54	0.54	0
	$h = 1$	0.76	0.52	0.24	0.76	0.52	0.24	0.36	0.36	0	0.53	0.53	0
	$h = 5$	0.81	0.75	0.06	0.67	0.56	0.11	1.1	1.1	0	0.24	0.23	0.01
	$h = 10$	0.80	0.75	0.05	0.61	0.52	0.09	0.09	0.09	0	0.71	0.71	0
NON	$h = 0$	0.70	0.50	0.20	0.93	0.50	0.43	0.44	0.43	0.01	0.79	0.48	0.31
	$h = 1$	0.72	0.52	0.20	0.93	0.52	0.41	0.40	0.38	0.02	0.69	0.50	0.19
	$h = 5$	0.79	0.78	0.01	0.84	0.56	0.28	1.1	1.1	0	0.33	0.25	0.08
	$h = 10$	0.91	0.91	0	0.79	0.55	0.24	0.96	0.96	0	0.85	0.85	0

information about nonlinear properties just as the magnitude series. It is not difficult to understand that the clustering of the same sign and clustering of large and small magnitude values appear simultaneously (Fig. 2(b)), as there are much more large-scale structures in the non-stationary time series, such that sign time series show evidently different nonlinear correlation properties between the stationary and non-stationary time series at large scales.

3.3. Correlations in multi-scale velocity increment

Multi-scale entropy analyses (MSE) have been used to quantify the differences between stationary and non-stationary traces [26]. Since different multi-scale increments can differentiate the different size eddy motions in the atmospheric surface layer [45], how the magnitude and sign correlations change with increment lags increasing for both stationary and non-stationary velocity time series deserves our further investigation. Here for scale factor $h = 1, 5, 10$, Fig. 5 shows how the magnitude and sign correlations change with changing h. For the magnitude series (Fig. 5(a)) and sign series (Fig. 5(b)), with the increment scale factor increasing, we can see the difference between the stationary and non-stationary series becomes smaller in accordance with multi-scale entropy analysis [26]; the nonlinearity if exists ($\Delta\alpha > 0$) decreases in the magnitude and sign time series of multi-scale velocity increment, diminishing even to zero ($\Delta\alpha = 0$) as shown in Table 1. The results show that the nonlinear correlation decreases ($\Delta\alpha$ decreasing) and the effects of non-stationarity on magnitude and sign scaling weaken as increment scale factor is increasing.

4. Discussions and conclusion

In this paper, we study the magnitude and sign scaling properties of multi-scale increment series from stationary and non-stationary vertical velocity records. With the help of series decomposition, we show the effect of non-stationarity on the magnitude and sign scaling properties of multi-scale velocity increment series.

Firstly, we show it is difficult to find a significant scaling range for stationary vertical velocity records themselves. In the log–log plot, the fluctuation function varies with window scale as a parabola function, so the fitting exponents over an insignificant scaling range are with great uncertainty. And there are two scaling ranges with different scaling exponents for

the original non-stationary data. Over the smaller scale range $s < s_x$, the scaling exponent is 1.45, and within the larger scale range $s > s_x$ the value of the scaling exponent is 0.89. Previous studies [17–19] on the original wind velocity records directly do not distinguish the stationary velocity records from the non-stationary ones, their results may be a mixed one from both cases. From their DFA results [17,18], we cannot find a dominant scaling range which exceeds one decade. In fact, they are more close to the results as we show for the stationary records in Fig. 3.

Secondly, for the increment series with lag one, the magnitude and sign scaling take different behaviors between stationary and non-stationary vertical velocity records. The nonlinear correlation found in magnitude fluctuations (i.e. volatility fluctuations) is obvious for both stationary and non-stationary cases, and there is only one scaling range which exceeds two decades for stationary case, see Fig. 4(a), but there are two scaling ranges over small and large scales for non-stationary case, where the dominant scaling range exceeds more than one decade, see Fig. 4(b). Similar results have been reported by Ref. [19], though they did not classify the type of the wind records. The linear correlation usually assumed to be found in the sign series takes two scaling ranges over small and large scales for both stationary and non-stationary cases. And over the smaller scale range, the linear correlation is the same for both stationary and non-stationary cases. However, over the larger scale range, the difference is sharp between stationary and non-stationary cases. And it is found that significant nonlinear correlation is also incorporated for the non-stationary case. Long-term correlation in the magnitude series indicates that an increment with large magnitude is more likely to be followed by an increment with large magnitude. Anti-correlation in the sign series indicates that a positive increment is more likely to be followed by a negative increment. Our result suggests that, in stationary time series a large increment in the positive direction is more likely to be followed by a large increment in the negative direction, whereas by a large increment in the positive direction for the non-stationary case at large scales.

Thirdly, with the lags in increment increasing, there exist two scaling ranges in both the magnitude and sign fluctuations for both stationary and non-stationary cases. For magnitude fluctuations, the nonlinear correlation over both small and large scale ranges will decrease with the lags increasing. For the sign series, the linear correlation is dominant over both small and large scale ranges for stationary case; the linear correlation is also dominant over small scale ranges for non-stationary case, the nonlinear correlation can be found over the large scale range for non-stationary case and will decrease with lags increasing. The nonlinear correlation found in the sign series over large scale range is resulted from the modulation of the large scale structures found in the non-stationary cases [26], which will incorporate parts of magnitude information into the sign series.

Acknowledgment

The authors acknowledge the supports from National Natural Science Foundation of China (No. 40975027).

References

[1] Y. Ashkenazy, P.C. Ivanov, S. Havlin, C.K. Peng, A.L. Goldberger, H.E. Stanley, Magnitude and sign correlations in heartbeat fluctuations, Phys. Rev. Lett. 86 (9) (2001) 1900–1903.
[2] C.K. Peng, S.V. Buldyrev, S. Havlin, et al., Mosaic organization of DNA nucleotides, Phys. Rev. E 49 (2) (1994) 1685–1689.
[3] M.S. Taqqu, V. Teverovsky, W. Willinger, Estimators for long-range dependence: an empirical study, Fractals 3 (04) (1995) 785–798.
[4] T. Kalisky, Y. Ashkenazy, S. Havlin, Volatility of linear and nonlinear time series, Phys. Rev. E 72 (1) (2005) 011913.
[5] S. Buldyrev, A. Goldberger, S. Havlin, et al., Long-range correlation properties of coding and noncoding DNA sequences: GenBank analysis, Phys. Rev. E 51 (5) (1995) 5084.
[6] J.W. Kantelhardt, Y. Ashkenazy, P.C. Ivanov, et al., Characterization of sleep stages by correlations in the magnitude and sign of heartbeat increments, Phys. Rev. E 65 (5) (2002) 051908.
[7] S. Bahar, J. Kantelhardt, A. Neiman, H. Rego, D. Russell, L. Wilkens, A. Bunde, F. Moss, Long-range temporal anti-correlations in paddlefish electroreceptors, EPL 56 (3) (2001) 454.
[8] J.M. Hausdorff, S.L. Mitchell, R. Firtion, et al., Altered fractal dynamics of gait: reduced stride-interval correlations with aging and Huntington's disease, J. Appl. Physiol. 82 (1) (1997) 262–269.
[9] E. Koscielny-Bunde, A. Bunde, S. Havlin, et al., Indication of a universal persistence law governing atmospheric variability, Phys. Rev. Lett. 81 (3) (1998) 729–732.
[10] P. Talkner, R.O. Weber, Power spectrum and detrended fluctuation analysis: application to daily temperatures, Phys. Rev. E 62 (1) (2000) 150–160.
[11] F. Lu, N. Yuan, Z.T. Fu, J. Mao, Universal scaling behaviors of meteorological variables' volatility and relations with original records, Physica A 391 (20) (2012) 4953–4962.
[12] B.D. Malamud, D.L. Turcotte, Self-affine time series: measures of weak and strong persistence, J. Statist. Plann. Inference 80 (1) (1999) 173–196.
[13] K. Ivanova, M. Ausloos, E. Clothiaux, T. Ackerman, Break-up of stratus cloud structure predicted from non-Brownian motion liquid water and brightness temperature fluctuations, EPL 52 (1) (2000) 40.
[14] C. Alados, M. Huffman, Fractal long-range correlations in behavior sequences of wild chimpanzees: a non-invasive analytical tool for the evaluation of health, Ethology 106 (2) (2000) 105–116.
[15] Y. Liu, P. Cizeau, M. Meyer, et al., Correlations in economic time series, Physica A 245 (3) (1997) 437–440.
[16] N. Van de walle, M. Ausloos, M. Houssa, et al., Non-Gaussian behavior and anti-correlations in ultrathin gate oxides after soft breakdown, Appl. Phys. Lett. 74 (11) (1999) 1579–1581.
[17] R.G. Kavasseri, R. Nagarajan, Evidence of crossover phenomena in wind-speed data, IEEE Trans. Circuits Syst. I. Regul. Pap. 51 (11) (2004) 2255–2262.
[18] R.G. Kavasseri, R. Nagarajan, A qualitative description of boundary layer wind speed records, Fluct. Noise Lett. 06 (02) (2006) L201–L213.
[19] R.B. Govindan, H. Kantz, Long-term correlations and multifractality in surface wind speed, EPL 68 (2) (2004) 184–190.
[20] Z. Chen, P.C. Ivanov, K. Hu, H.E. Stanley, Effect of nonstationarities on detrended fluctuation analysis, Phys. Rev. E 65 (4) (2002) 041107.
[21] N. Cullen, K. Steffen, P. Blanken, Nonstationarity of turbulent heat fluxes at Summit, Greenland, Bound.-Layer Meteorol. 122 (2) (2007) 439–455.
[22] L. Mahrt, C. Thomas, S. Richardson, N. Seaman, D. Stauffer, M. Zeeman, Non-stationary generation of weak turbulence for very stable and weak-wind conditions, Bound.-Layer Meteorol. 147 (2013) 179.
[23] K.R. Sreenivasan, A. Bershadskii, Clustering properties in turbulent signals, J. Stat. Phys. 125 (2006) 1141.

[24] D. Cava, G.G. Katul, The effects of thermal stratification on clustering properties of canopy turbulence, Bound.-Layer Meteorol. 130 (3) (2009) 307–325.
[25] Q.L. Li, Z.T. Fu, The effects of non-stationarity on clustering properties of boundary layer vertical wind velocity, Bound.-Layer Meteorol. 149 (2) (2013) 219–230.
[26] Z.T. Fu, Q.L. Li, N. Yuan, Z. Yao, Multi-scale entropy analysis of vertical wind variation series in atmospheric boundary-layer, Commun. Nonlinear Sci. Numer. Simul. 19 (1) (2013) 83–91.
[27] Q.L. Li, N. Ma, Z.T. Fu, Comparative analysis of detection methods of non-stationarity in time series, Acta Sci. Natur. Univ. Pekinensis 49 (2) (2013) 252–260.
[28] D.J. Yu, W.P. Lu, R.G. Harrison, Space time-index plots for probing dynamical nonstationarity, Phys. Lett. A 250 (4–6) (1998) 323–327.
[29] D.J. Yu, W.P. Lu, R.G. Harrison, Detecting dynamical nonstationarity in time series data, Chaos 9 (4) (1999) 865–870.
[30] Y. Ashkenazy, P.C. Ivanov, S. Havlin, C.K. Peng, Y. Yamamoto, A.L. Goldberger, H.E. Stanley, Decomposition of heartbeat time series: scaling analysis of the sign sequence, Comput. Cardiol. 2000 (2000) 139–142.
[31] Y. Ashkenazy, S. Havlin, P.C. Ivanov, C.K. Peng, V. Schulte-Frohlinde, H.E. Stanley, Magnitude and sign scaling in power-law correlated time series, Physica A 323 (2003) 19–41.
[32] V. Livina, Y. Ashkenazy, P. Braun, et al., Nonlinear volatility of river flux fluctuations, Phys. Rev. E 67 (4) (2003) 042101.
[33] K. Hu, P.C. Ivanov, et al., Non-random fluctuations and multi-scale dynamics regulation of human activity, Physica A 337 (1–2) (2004) 307–318.
[34] P. Ivanov, A. Yuen, Z. Chen, et al., Common scaling patterns in intertrade times of U.S. stocks, Phys. Rev. E 69 (5) (2004) 056107.
[35] B. Podobnik, P. Ivanov, K. Biljakovic, et al., Fractionally integrated process with power-law correlations in variables and magnitudes, Phys. Rev. E 72 (2) (2005) 026121.
[36] L. Zhu, N.D. Jin, Z.K. Gao, et al., Magnitude and sign correlations in conductance fluctuations of horizontal oil water two-phase flow, J. Phys. Conf. Ser. 364 (2012) 012067.
[37] T. Schreiber, A. Schmitz, Improved surrogate data for nonlinearity tests, Phys. Rev. Lett. 77 (4) (1996) 635–638.
[38] J. Chen, F. Hu, Coherent structures detected in atmospheric boundary-layer turbulence using wavelet transforms at Huaihe River Basin, China, Bound.-Layer Meteorol. 107 (2) (2003) 429–444.
[39] H. Chen, J. Chen, F. Hu, Q. Zeng, The coherent structure of water vapor transfer in the unstable atmospheric surface layer, Bound.-Layer Meteorol. 111 (3) (2004) 543–552.
[40] X. Li, F. Hu, G. Liu, Characteristics of chaotic attractors in atmospheric boundary-layer turbulence, Bound.-Layer Meteorol. 99 (2) (2001) 335–345.
[41] J. Wang, Z. Fu, L. Zhang, S. Liu, Information entropy analysis on turbulent temperature series in the atmospheric boundary-layer, Plateau Meteorology. 24 (1) (2005) 38–42.
[42] C.K. Peng, S. Havlin, H.E. Stanley, A.L. Goldberger, Quantification of scaling exponents and crossover phenomena in nonstationary heartbeat time series, Chaos 5 (1) (1995) 82–87.
[43] B. Podobnik, D.F. Fu, H.E. Stanley, P.C. Ivanov, Power-law autocorrelated stochastic processes with long-range cross-correlations, Eur. Phys. J 56 (1) (2007) 47–52.
[44] K. Hu, P.C. Ivanov, Z. Chen, P. Carpena, H.E. Stanley, Effect of trends on detrended fluctuation analysis, Phys. Rev. E 64 (1) (2001) 011114.
[45] K. Wesson, G. Katul, M. Siqueira, Quantifying organization of atmospheric turbulent eddy motion using nonlinear time series analysis, Boundary -Layer Meteoro 106 (3) (2003) 507–525.